

# Anisotropy engineering in Co nanodiscs fabricated using prepatterned silicon pillars

C Thirion<sup>1</sup>, W Wernsdorfer<sup>1</sup>, M Kläui<sup>2</sup>, C A F Vaz<sup>3</sup>, P Lewis<sup>3</sup>,  
H Ahmed<sup>3</sup>, J A C Bland<sup>3</sup> and D Maily<sup>4</sup>

<sup>1</sup> Laboratoire Louis Néel, associé à l'UJF, CNRS, BP 166, 38042 Grenoble Cedex 9, France

<sup>2</sup> Fachbereich Physik, Universität Konstanz, Universitätsstrasse 10, D-78457 Konstanz, Germany

<sup>3</sup> Cavendish Laboratory, University of Cambridge, UK

<sup>4</sup> LPN, CNRS, Route de Nozay, 91460 Marcoussis, France

## Abstract

Magnetic nanodiscs are fabricated by depositing cobalt onto 10–30 nm diameter silicon nanopillars, which were prepatterned using gold colloids as etch masks. The magnetic anisotropy energy of individual nanodiscs is studied by measuring the angular dependence of switching field using the micro-SQUID technique. The Stoner–Wohlfarth model, describing the magnetization reversal by uniform rotation, is used to analyse the data. The switching astroids of pure Co exhibit a cubic magnetocrystalline anisotropy indicating that the Co crystallites are fcc. After controlled oxidation of the nanoparticles, the anisotropy is dominated by a defect-induced uniaxial anisotropy, which means that the anisotropy can be used as a quality gauge.

Understanding and engineering magnetic anisotropies is critically important in magnetic nanostructures, since they govern both the static and dynamic physical properties of such systems. The effective anisotropy, which determines the easy and hard magnetization directions is a superposition of different contributions including magnetocrystalline, surface and shape anisotropy [1]. Some of these terms can be tailored, such as the magnetocrystalline anisotropy by choosing the material and the shape anisotropy by selecting a geometry. Other anisotropy terms are related to defects, such as misfit dislocations and local oxidation spots. These anisotropies tend to be uniaxial, while the other ones can be engineered to be of higher order, such as cubic. A direct measurement of the individual anisotropy contributions is usually not possible in nanoparticle systems. However, the entire anisotropy function is measurable via the three-dimensional critical surface of the switching fields [2]. Since our measurement of the famous Stoner–Wohlfarth astroid [3] on a single nanoparticle, we have investigated different particles from 40 nm barium ferrite to 3 nm cobalt nanoparticles [4–8]. One of the intriguing questions that emerged when we tried to engineer the anisotropies was why the observed anisotropies always had a prevalent uniaxial anisotropy. This observation was

contrary to expectations that small fcc Co particles, which we studied, should exhibit a pure cubic magnetocrystalline anisotropy. For applications, the key task is designing anisotropies, since for applications such as memory devices, the anisotropies determine the minimum bit size which is thermally stable [9, 10]. Such design is possible if the anisotropy is determined by the choice of materials and crystallographic phase rather than by defects, which are inherently hard to control. Thus the key question is whether the observed uniaxial anisotropy stems from defects or whether it corresponds to the inherent anisotropy of the system. To unambiguously demonstrate that the anisotropies can be engineered in single domain particles, and are not defect dominated, a system has to be devised which exhibits a pure higher-order anisotropy. Even for the simplest case, which is the cubic anisotropy, so far no results on single domain particles that exhibit a purely or at least dominating cubic anisotropy have been made available.

In this paper, we present an experimental study of the anisotropy of single cobalt nanodiscs that were fabricated on prepatterned silicon, and a comparison with theoretical predictions. We probe to what extent the anisotropies observed coincide with the engineered anisotropies, and we propose that

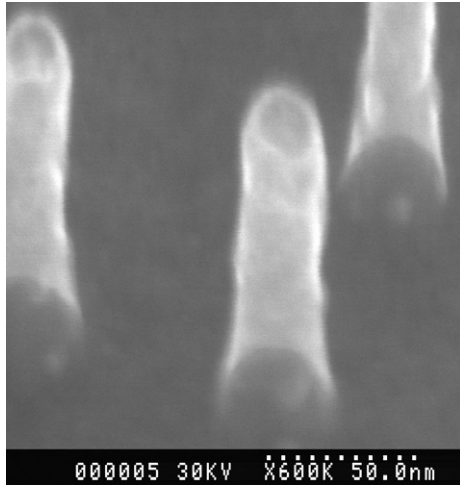


**Figure 1.** SEM image of a 120 nm tall prepatterned Si nanopillar after removing the 30 nm Au colloids used as etch masks. They exhibit a circular top with a good edge definition

the measured anisotropy can be used as a ‘quality factor’ to estimate the influence of defects in the nanoparticle.

To fabricate high quality single domain particles, we have devised a method which uses pre-patterned semiconductor substrates as templates for growth of magnetic nanostructures. Previous experiments on larger structures (>200 nm) show that high quality epitaxial fcc Co elements with a cubic magneto-crystalline anisotropy can be fabricated using this technique [11, 12]. Although the minimum feature size that can be lithographically defined is limited by the electron beam resolution, the use of subsequent anisotropic etching means that elements can be obtained after etching that are smaller than that which was defined after the lithography [11]. To go beyond the resolution of electron-beam lithography, we have used gold colloids (10–30 nm diameter) as etch masks. For the experiments reported here, 30 nm diameter gold particles were deposited on Si(001) substrates. The colloidal gold particles were deposited using an amino-silane adhesion agent to obtain a layer of isolated gold particles. Using the colloidal gold as an etch mask, the silicon nanopillars were fabricated with a  $\text{SiCl}_4$  based reactive ion etching to form nanopillars with only a small undercut [13]. The colloidal gold etch masks were then stripped using an aqua regia wet etch. For 30 nm Au colloids, scanning electron microscopy (SEM) revealed the nanopillars to be approximately 120 nm tall with a diameter of  $\sim 25$  nm (an example is shown in figure 1). After patterning of the semiconductor substrate into nanopillars, the 5–15 nm thick Co layers are grown with molecular beam epitaxy. The growth on top of the nanopillars leads to the formation of nanodiscs. These were fully coated with a gold layer by depositing the gold at an angle while rotating the sample. The details of the growth are described in [14].

We studied the magnetization reversal of individual nanodiscs by using planar Nb micro-bridge-DC-SQUIDS at 30 mK [4]. A  $2 \text{ mm} \times 2 \text{ mm}$  substrate with nanodiscs on nanopillars was attached on top of a chip with an array of micro-SQUIDS. The latter can detect the magnetization reversal of a single nanodisc for an applied magnetic field in any direction. However, the desired sensitivity is only achieved

for nanodiscs which are very close to the microbridges, where the magnetic flux coupling is high. Statistically only a few nanodiscs are close to the microbridge of the SQUID. In many cases, only one nanodisc gave a measurable signal. For cases with several signals, a precise study allowed us to show that each signal corresponds to an independent nanodisc. Indeed, by studying the intersection of two Stoner–Wohlfarth astroids we were able to determine the strength of the interaction between particles, which was found to be negligible. Experimental details of the measuring technique are given elsewhere [15].

Figures 2(a)–(c) display three typical angle dependences of the switching fields of 30 nm wide and 15 nm thick Co nanodiscs. An example of a nearly perfectly cubic anisotropy as shown in figure 2(a). Figure 2(b) exhibits a mixture of cubic and uniaxial anisotropy contributions, and figure 2(c) a nearly uniaxial anisotropy. We used the Stoner–Wohlfarth model of uniform rotation of magnetization [3] in order to analyze the experimental results.

The model of uniform rotation of magnetization, developed by Stoner and Wohlfarth [3] and Néel [16], is the simplest classical model describing magnetization reversal. One considers a particle of an ideal magnetic material where exchange energy holds all spins tightly parallel to each other, and the magnetization magnitude does not depend on space. In this case the exchange energy is constant, and it plays no role in the energy minimization. Consequently, there is competition only between the effective anisotropy energy of the particle and the effect of the applied magnetic field. The original model of Stoner and Wohlfarth assumed only uniaxial shape anisotropy with one anisotropy constant—that is, one second-order term. This is sufficient to describe highly symmetric cases like a prolate spheroid of revolution or an infinite cylinder. However, real systems are often quite complex, and the anisotropy is a sum of mainly shape (magnetostatic), magnetocrystalline, magnetoelastic, and surface anisotropy. One additional complication arises because the different contributions to the anisotropy are often aligned in an arbitrary way with respect to each other. All of these facts motivated a generalization of the Stoner–Wohlfarth model for an arbitrary effective anisotropy by Thiaville [2].

One supposes that the exchange interaction in a nanodisc couples all the spins strongly together to form a giant spin whose direction is described by the unit vector  $\vec{m}$ . The only degrees of freedom of the particle’s magnetization are the two angles of orientation of  $\vec{m}$ . The reversal of the magnetization is described by the free Gibbs energy (in reduced units):

$$V_{\vec{h}}(\vec{m}) = G(\vec{m}) - 2\vec{h}, \quad (1)$$

where  $G(\vec{m})$  is the effective anisotropy function and  $\vec{h}$  the reduced applied field. In order to describe our experimental results (figure 2), we take into account the cubic magnetocrystalline anisotropy and a uniaxial anisotropy term and both anisotropies might be misaligned. Thus, the simplest effective anisotropy function for our nanodisc is given by:

$$G(\vec{m}) = \vec{m}^T K \vec{m} + K_c(m_x^2 m_y^2 + m_y^2 m_z^2 + m_z^2 m_x^2) \quad (2)$$

where  $K$  is the second-order anisotropy tensor and  $K_c$  is the cubic anisotropy constant. A fit of our data in the  $xy$ -plane

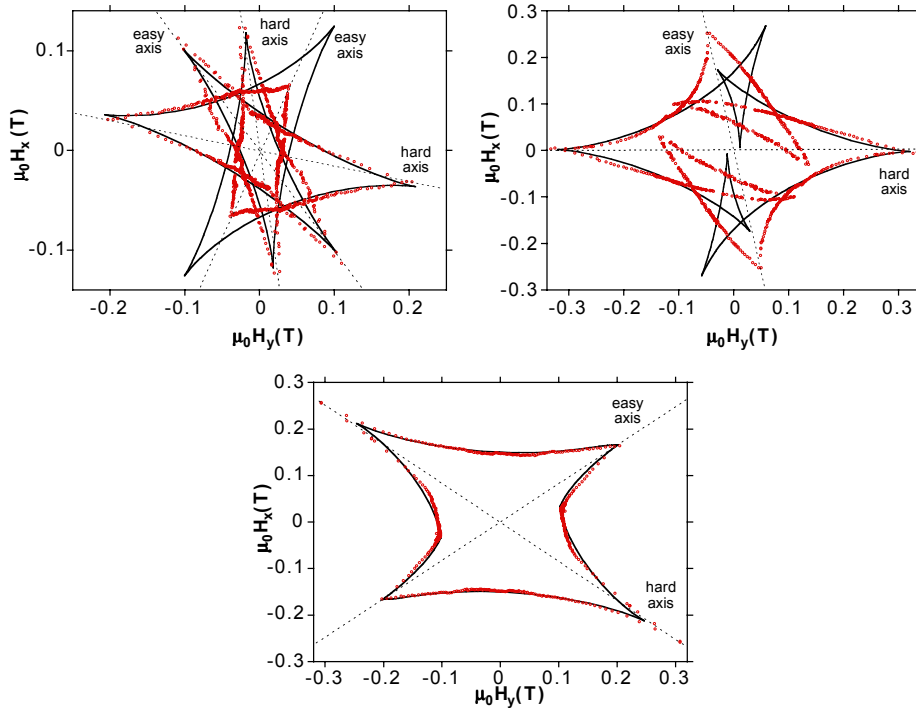


**Figure 2.** Angle dependence of the switching field of three Co nanodiscs at 0.04 K. The magnetic anisotropies are: (a) cubic (top left); (b) mixture of cubic and uniaxial (top right); and (c) uniaxial (bottom). The easy and hard axes of magnetization are indicated. The continuous line is a fit using the following parameters: (a)  $K_{xx} = 0$ ,  $K_{yy} = 0.01$  T,  $K_{zz} = 1$  T,  $K_{xy} = 0$  T,  $K_{yz} = 0$ ,  $K_{xz} = 0$ ,  $K_c = -0.25$  T. The principal axes of the cubic term are rotated by the Euler angles  $(\psi, \theta, \phi)_c = (21^\circ, 57^\circ, -12^\circ)$  and the entire anisotropy function is rotated by  $(\psi, \theta, \phi)_{SQ} = (13^\circ, 142^\circ, 144^\circ)$ . (b)  $K_{xx} = -0.02$ ,  $K_{yy} = 0.2$  T,  $K_{zz} = 0.8$  T,  $K_{xy} = -0.015$  T,  $K_{yz} = -0.2$ ,  $K_{xz} = -0.08$ ,  $K_c = -0.25$  T,  $(\psi, \theta, \phi)_c = (54^\circ, 14^\circ, 18^\circ)$ ,  $(\psi, \theta, \phi)_{SQ} = (70^\circ, 30^\circ, 41^\circ)$ , and (c)  $K_{xx} = 0$ ,  $K_{yy} = 0.204$  T,  $K_{zz} = 0.33$  T,  $K_{xy} = 0.065$  T,  $K_{yz} = 0$ ,  $K_{xz} = 0$ ,  $K_c = -0.1$  T,  $(\psi, \theta, \phi)_c = (-6^\circ, 6^\circ, -5^\circ)$ ,  $(\psi, \theta, \phi)_{SQ} = (5^\circ, 6^\circ, -66^\circ)$ . (This figure is in colour only in the electronic version)

is presented by the continuous lines in figure 2(a)–(c). The anisotropy constants  $K$  are given in tesla and can be readily converted to energy densities:  $K_{\text{energy-density}} = KM_s$  ( $M_s = 1.45 \times 10^6$  A m<sup>-1</sup>).  $K_{zz}$  was supposed to be large because the nanodiscs are flat film elements leading to large dipolar field that try to keep the magnetization in the plane of the nanodisc. The exact value of  $K_{zz}$  was not important for the fits. The principal cubic axes were found to be slightly rotated out of the  $xy$ -plane. This might be due to a small tilting of the pillars in respect to the substrate plane caused by our positioning technique onto the SQUID array. It can be seen that we have been able to fit the cubic and the uniaxial astroids very well by the Stoner–Wohlfarth theory, since in that case we have one dominating anisotropy contribution. For the intermediate case (figure 2(b)) such a fit is more difficult due to the complex interplay between the uniaxial and the cubic anisotropy terms yielding a more complicated astroid.

We demonstrate here that some of the discs exhibit a predominant cubic term (figure 2(a)) with a cubic anisotropy constant similar to that measured on fcc Co films [17], which indicates that we indeed measure circular fcc Co nanodiscs with a cubic magnetocrystalline anisotropy. The absence of a strong uniaxial term in nanopillar structures suggests that we have engineered the anisotropy by choosing a material with a cubic anisotropy and a structure which shows no significant defects, such as oxidation, geometrical irregularities or stacking faults in the crystal. A possible reason is that

this fabrication method (growth on prepatterned Si nanopillars) gives a very good edge definition (see figure 1) and seems to be less prone to shape variations. These results confirm the high-quality UHV growth of the Co nanodiscs.

To further elucidate the influence of defects, we have let the samples oxidize in air for a month. When remeasuring the same sample, all of the particles turned out to exhibit a uniaxial anisotropy as shown in figure 2(c). This further corroborates the finding that the strength of the cubic anisotropy as compared to the uniaxial contribution can be used as a ‘quality factor’ to judge the importance of defects in a particle. From this we can also infer that the uniaxial anisotropy observed in other systems, where a cubic anisotropy is expected, is likely to originate from defects.

In conclusion, we presented switching field measurements as a function of the angle of the applied field for single nanodiscs, which allowed us to determine the effective magnetic anisotropy function of cobalt nanodiscs. Some of these nanoparticles showed that we have been able to engineer a cubic anisotropy, allowing us to measure a cubic astroid. This suggests that the versatile fabrication method used yields nanodiscs with a very high shape and crystalline quality, which opens up a way to engineer other anisotropies by e.g. varying the materials. Controlled oxidation leads to a predominant uniaxial anisotropy, which allows us to conclude that the anisotropy can be used to gauge the sample quality.

## Acknowledgments

We thank A Thiaville for helpful discussions. Part of this work was supported by DRET, Rhône-Alpes, the MASSDOTS ESPRIT LTR-Project No 32464, the EPSRC (UK), the Deutsche Forschungsgemeinschaft (SFB 513) and the Landesstiftung Baden Württemberg.

## References

- [1] Hubert A and Schäfer R 1998 *Magnetic Domains. The Analysis of Magnetic Microstructures* (Berlin-Heidelberg-New York: Springer)
- [2] Thiaville A 1998 *J. Magn. Magn. Mater.* **182** 5  
Thiaville A 2000 *Phys. Rev. B* **61** 12221
- [3] Stoner E C and Wohlfarth E P 1948 *Phil. Trans. A* **240** 599
- [4] Wernsdorfer W, Bonet Orozco E, Hasselbach K, Benoit A, Barbara B, Demoncey N, Loiseau A, Pascard H and Maily D 1997 *Phys. Rev. Lett.* **78** 1791
- [5] Wernsdorfer W, Bonet Orozco E, Hasselbach K, Benoit A, Maily D, Kubo O, Nakano H and Barbara B 1997 *Phys. Rev. Lett.* **79** 4014
- [6] Bonet E, Wernsdorfer W, Barbara B, Benoit A, Maily D and Thiaville A 1999 *Phys. Rev. Lett.* **83** 4188
- [7] Jamet M, Wernsdorfer W, Thirion C, Maily D, Dupuis V, Mélinon P and Pérez A 2001 *Phys. Rev. Lett.* **86** 4676
- [8] Wernsdorfer W, Thirion C, Demoncey N, Pascard H and Maily D 2002 *J. Magn. Magn. Mater.* **242–245** 132
- [9] Prinz G A 1999 *J. Magn. Magn. Mater.* **200** 57
- [10] Hadjipanayis G C 2001 *Magnetic Storage Systems Beyond 2000* (Dordrecht: Kluwer–Academic)
- [11] Rothman J, Kläui M, Lopez-Diaz L, Vaz C A F, Bleloch A, Bland J A C, Cui Z and Speaks R 2001 *Phys. Rev. Lett.* **86** 1098
- [12] Vaz C A F, Lopez-Diaz L, Kläui M, Bland J A C, Monchesky T L, Unguris J and Cui Z 2003 *Phys. Rev. B* **67** 140405(R)
- [13] Lewis P *et al* 1999 *J. Vac. Sci. Technol. B* **17** 3239
- [14] Kläui M, Lewis P A, Vaz C A F, Bleloch A, Speaks R, Bland J A C and Ahmed H 2002 *Microelectron. Eng.* **61/62** 593600
- [15] Wernsdorfer W 2001 *Adv. Chem. Phys.* **118** 99
- [16] Néel L 1947 *C. R. Acad. Sci.* **224** 1550
- [17] Krams P, Lauks F, Stamps R L, Hillebrands B and Guntherodt G 1992 *Phys. Rev. Lett.* **69** 3674